Available online at http://scik.org
Commun. Math. Biol. Neurosci. 2021, 2021:6
https://doi.org/10.28919/cmbn/5276
ISSN: 2052-2541

SOME ASPECTS OF FLUCTUATIONS DYNAMICS OF PARTICLES IN DUSTY PLASMA

S. S. SAFAAI[1,*], S. L. YAP[1], S. V. MUNIADY[1], M. AYAZ AHMAD[2]

[1]Faculty of Science, Plasma Technology Research Centre, University of Malaysia, Kuala Lumpur, Malaysia

[2]Department of Physics, Faculty of Science, P. O. Box741, University of Tabuk, 71491, Saudi Arabia

Abstract. Dusty plasmas are formed when micrometre particles of solid matter are introduced into glow discharge plasma. In the present research work, we investigated the fluctuation dynamics of the particles using the dynamic light scattering (DLS) technique and particle tracking with high-speed imaging technique. The DLS technique gives light intensity fluctuation which is analysed by fractal tools namely wavelet scalogram to give the Hurst parameter, "H" being associated with the fractional Brownian motion. The structural phases of particles are analysed using the pair correlation function. Particle trajectory analysis determines the transport characteristics of the charged dust particles. The scaling behaviour of the mean squared displacement (MSD) is investigated for different pressures. Results from both the DLS and MSD analysis are discussed regarding different transport mechanisms based on the fractional Brownian motion as the transport model. This study also highlighted the use of fractal analysis as a powerful tool for investigating fluctuation dynamics in dusty plasmas.

Keywords: particle tracking; dynamic light scattering (DLS) technique; dusty plasma; DLS and MSD analysis and scalogram.

2010 AMS Subject Classification: 00A06, 00A79.

[*]Corresponding author
E-mail addresses: ctsarah1001@gmail.com, sarahsafaai@utm.my
Received November 28, 2020

1. INTRODUCTION

Dusty plasma research is concerned with the interactions taking place between charged dust particles and plasma. Dusty plasma consists of electrons, ions, neutral gas atoms and additional microscopic particles, with sizes ranging from about 10 nm to several 10 micrometres. Typically, the additional particles are larger than other plasma particles attracting ions and electrons [1].

The dusty plasma may be considered as a complex system, due to the numerous interactions between dust particles, electrons, ions and neutral atoms. The collection of thousands of charged plasma species (for example electrons and ions) on dust particle surface cause the dust particles to carry large amount charge, hence induce strong Coulomb interaction. The charged dust particles not only alter the composition of plasma but also trigger new physical processes on the systems.

Research on dusty plasma has covered different areas including the fundamental aspects of plasma physics, hydrodynamic, nonlinear physics, kinetics of phase transitions and solid state [1]. It also includes dynamics of dust-plasma dust particles [2], collective dynamics [3], self-organisation [4] and many other nonlinear processes [5]. The experiments concerning complex plasma diffusion as reported by [6], marks one of the primary studies conducted on this topic.

This paper is inspired by the fact that fluctuation is ubiquitous in a variety of complex systems including complex plasmas such as dusty plasma. Among the common features of fluctuation dynamics is the fractal properties with power-law scaling properties. A typical example originating from plasma related phenomenon is the lightning process with the fractal pattern. Fractal modelling also found application in economics, geography, physics and biology that exhibit scale invariance or self-similarity behaviour. Fractal behaviours can be seen in the spatial patterns such as trajectories of Brownian motion of dust particle or variation of relevant physical quantities such as position, temperature or current as a function of time, hence known as fractal signals and can be modelled using fractal stochastic processes.

Fractal scaling behaviour in fluctuation of various physical quantities related to plasmas and dusty plasmas have been reported in a number of studies. For example, fluctuation in floating potential glow discharge was reported by Nurujjaman *et al*. [7], and in tokamak edge by Zajac *et al* [8]. Some literature of scaling behavior in the dusty plasmas are mostly focused on identifying the type of particle transport. It is capable of differentiating the normal and the anomalous diffusion using mean square displacement.

Recognizing this prospect has not been widely explored in the field of complex plasmas such as dusty plasmas, has serve as the motivation for this thesis. Based on the versalities and ease of applications to complex data, such as fluctuations, noisy time series and complex spatial patterns, we have applied a suite of fractals, multifractals, wavelets and information theoretic approaches to understand particle dynamics, fulfilling our first and second objectives. We have carried out detailed experiments involving two complementary approaches namely dynamic light scattering experiments and particle trajectory analysis and interpret the relevant scaling relations and the corresponding scaling exponents. Scaling exponents of power-law relations are signature of fractal or (time/spatial) scale invariance, which is the third objective of this study. Finally we have provided a consistent interpretation that link what may appear to be exclusive approaches, one observing indirectly the effect of particle motion via the scattered lights and another based on direct observation of the particle in real space and time domain. This answered the final objectives of the study. The details of the findings and their significances are discussed in the following section.

2. PARTICLE TRANSPORT IN DUSTY PLASMA

In the particle transport, the diffusion is one of the main interests. For example, the diffusion exponent is calculated from the scaling behaviour of particle trajectories [9]. An anomalous scaling often found in the liquid and crystal state of dusty plasma which indicates the different type of transport in the shorter time and longer time. A various technique to identify the type of transport such as; mean square displacement, velocity autocorrelation function and the probability distribution function. Super diffusion in the dusty plasma frequently reports by the Lin I group and Goree group [10,11]. However, Hou and Nonumura report they found the subdiffusion and no sign of super diffusion [9,12]. Ratynskaia used fractal analysis to calculate the Hurst exponent and suggest this approach overcome the difficulty in the anomalous scaling in means square displacement [13].

Other particle transport also has been actively investigated in dusty plasma laboratory and by computer simulation. The viscosity, diffusion constant and pair correlation function at different conditions in dusty plasma have been studied [14]. Experimental techniques using high speed camera and laser illumination in the microgravity experiment was carried out to study the transport coefficient and shear viscosity in a strongly coupled dusty plasma system [15]. Particle image velocimetry was used to obtain detailed measurements of particle transport and thermal state in dusty plasma [16].

The work of correlation analysis in dynamic light scattering have been carried to study the transport behaviour [17], correlation model [18], thermal energy [19], structure function [20] and particle growth [21]. The time series of scattered light carried information of charge particle indicate the intensity function is a long memory. Muniandy *et al*. demonstrates the fractional correlation model fit better than another convention model [18]. Comparing the dynamic light scattering (DLS) and particle visualization technique, Aschinger proved that the thermal energy of DLS in the phase transition of dusty plasma gives better results [19].

3. METHODOLOGY

In this work we have presented an empirical investigation of particle dynamics and fluctuation complex dusty plasma in 13.5 MHz radio-frequency capacitively coupled gas discharge systems. The observation of structural states was performed by varying the argon pressure discharge in the range of 0.1 mbar to 0.7 mbar with constant power at 50 W. Once the charged dust clouds are in equilibrium floating above the lower electrode, measurement intensity fluctuation from dynamic light scattering of particle were measured and at the same time the particle clouds are observed using high-speed video imaging system connected to the particle tracking software. Particle trajectories were constructed from the sequential image frames based on the video files.

The study was focused on the surface layer of the dust cloud with a diameter of 2.5 cm. The dust cloud was levitated by a high electric field that was formed by a small hole with a 5 mm depth of the lower electrode. The dynamics of the charged dust are affected by the power and pressure applied to the system. This includes the strength of Coulomb coupling between the charged dust particles through the kinetic energy via collisions of neutral atoms.

The height of the electric field is also affected by the pressure. The electric field regime is lowered as the pressure is increased. Based on other studies on dusty plasma system with similar experimental parameters, the charge number on the dust particles were reported to be in the range of $\mathrm{Q} = 10^3$ to 10^5. Meanwhile, the electron temperature was typically below 10 keV.

For visualization purposes, the dust particle motion was recorded using an EoSens CL high-speed-CMOS video camera running at a rate of 200 frames per second and equipped with a macro lens. The raw image obtained from the camera was shown in Figure 2. Particle tracking algorithm was implemented on the raw video data to obtain particles trajectories. Blair and Dufresne developed the particle tracking algorithm used in this work [22]. The algorithm search for the most probable particle location in the consecutive image frame based on the closest inter-particle distance. This will eventually allow us to construct the time series of particles' trajectories in two-dimension.

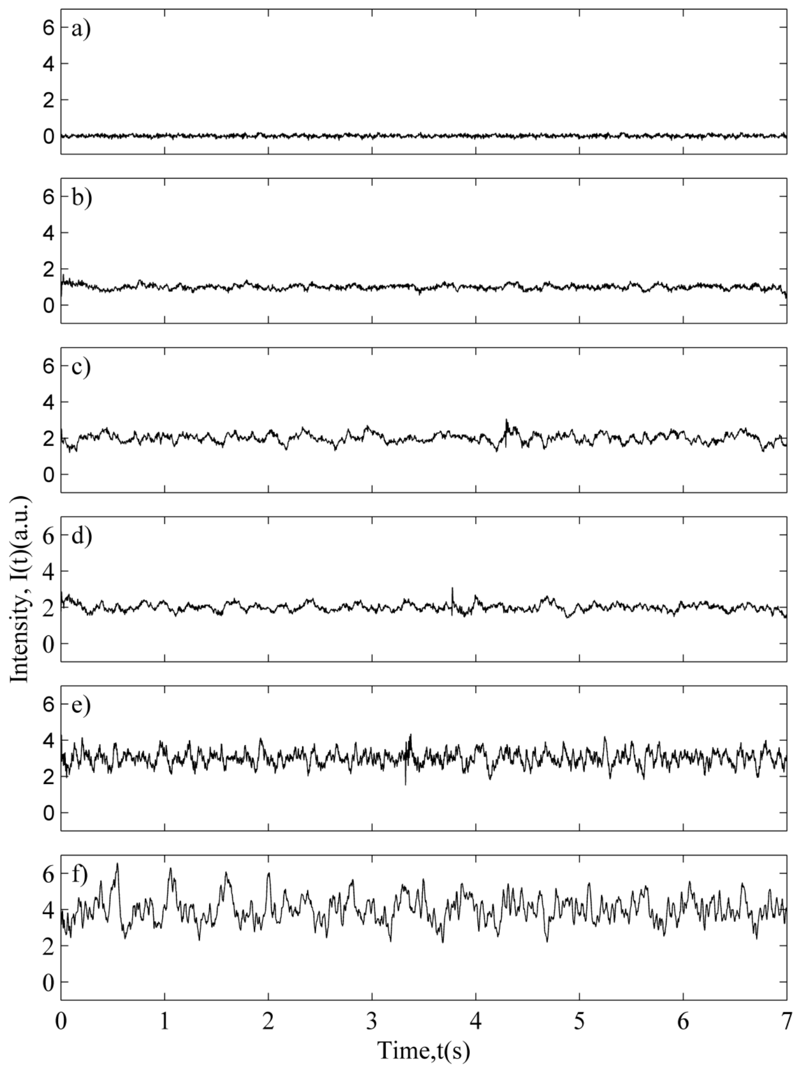

FIGURE 1. A pictorial depiction of the filtered time series of the light intensity fluctuation in the DLS signals such as; a) Dust off, b) 0.696 mbar, c) 0.592 mbar, d) 0.441 mbar, e) 0.292 mbar and f) 0.141 mbar repectively.

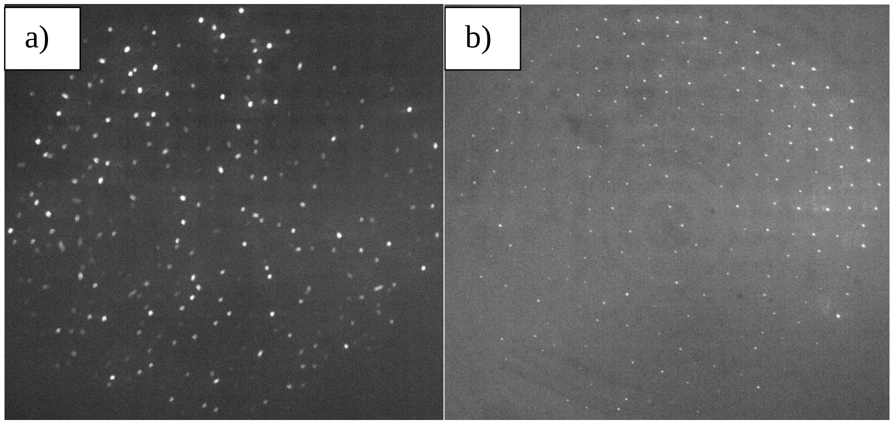

FIGURE 2. The raw image of the dust particles at a pressure; (a) at 0.141 mbar and (b) at 0.696 mbar respectively.

4. WAVELET ANALYSIS

Wavelet analysis is a robust tool for characterising the fractal scaling in fluctuation phenomena in the presence of non-stationary or trend. Referring to Section 3.2.4, Eq. (3.2.8), one can deduce the Hurst exponent from the power-law scaling exponent γ of the scalogram, namely $\gamma = 2H_W + 1$ (subscript W is used to differentiate the Hurst exponent obtained from PSD). Here once again similar to PSD, one assumes the fractal signal can be modelled as FBM, where γ indicates the slopes of the linear scaling regimes determined by using the linear least square fitting as shown in the inset of Figure 3. We used Daubechies wavelet (Db2) to calculate the discrete wavelet transform and eventually the discrete scalogram as function of scale parameter $a = 2^j$, with j is scale index or octave, The flat spectrum at a small-scale regime (or high frequency) for scale index $j \sim 1,\ldots,5$ represents the background noise present in all the time series. The background noise is found to be a non-scaling time series with relatively flat spectrum as one would expect of the non-scaling white noise. The background noise has been shown to satisfy the Gaussian statistics and temporal uncorrelated.

Compared to the previous analysis (PSD), the trend was similar to the graph can be divided into two regimes. The wavelet scalogram must be interpreted in a reciprocal way as compared to the power spectral analysis because the scale *a* is inversely proportional to frequency. Small scale implies a high frequency and vice versa. Thus, background noise was found in a small-scale regime, while the correlated signal was found in an intermediate to large-scale regime. Figure 3 shows the discrete scalogram obtained from discrete wavelet analysis. The power-law scaling regime in the plots will be used to determine the scaling exponents, hence the Hurst exponent using the relation described earlier. In the presence of dust, the power-law behaviour in a log-log plot of the wavelet scalogram is quite evident (indicating a monofractal behaviour), particularly in the scaling regimes having indices from j= 5 to j=11 (corresponding to the time scales 0.01s – 1s). The scaling exponents are determined from the gradient of this regime and summarized in Table 4.2. The wavelet scalogram analysis shows a significant difference in the scaling behaviour for lower pressure and higher pressure cases. The scalogram scaling exponent, γ for a gas pressure of 0.141 mbar is significantly higher (implying higher Hurst exponent) in comparison to the other DLS signals, which have almost comparable gradients (or spectral exponents) at higher pressures.

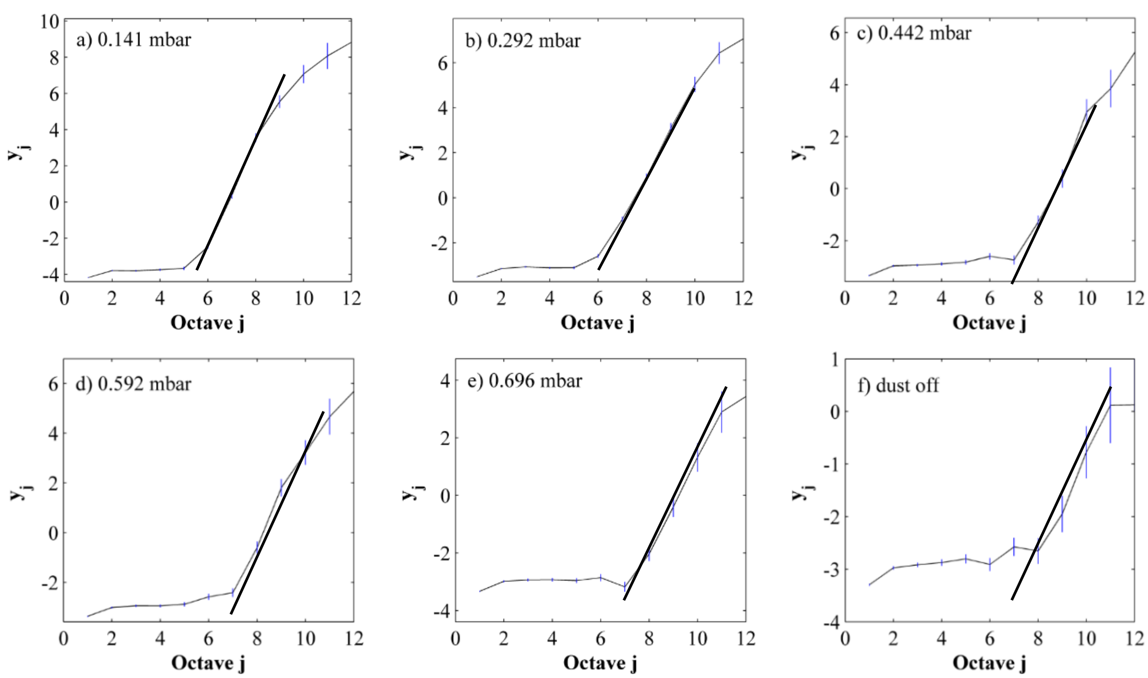

FIGURE 3. Wavelet scalograms of intensity fluctuation time series for different pressures.

The lowest pressure (0.141mbar) shows the largest scaling range and has the highest value of the Hurst exponent, $H_W = 0.81 \pm 0.02$ (persistent). The Hurst exponents of other higher pressures were lower than $H = 0.5$, which indicates that the signals displayed short-range dependence (anti-persistent) behaviours. The power-law scaling regime appears to be shifted as one increase the gas pressures. The lowest value of Hurst exponent $H_W = 0.25 \pm 0.04$ is obtained for the gas pressure of 0.696 mbar.

TABLE 1. The wavelet scalogram scaling exponents and the Hurst exponents for light intensity fluctuation analysis at different pressures.

Pressure (mbar)	**The range of scale index, *j***	**Scalogram Scaling Exponent, *γ***	**Wavelet-based Hurst exponent, H_W**
0.141 ± 0.001	5 - 10	0.81 ± 0.02	0.81 ± 0.02
0.292 ± 0.001	6 - 10	0.45 ± 0.01	0.45 ± 0.01
0.442 ± 0.001	7 - 11	0.36 ± 0.01	0.36 ± 0.01
0.592 ± 0.001	7 - 11	0.47 ± 0.02	0.47 ± 0.02
0.696 ± 0.001	7 - 11	0.25 ± 0.04	0.25 ± 0.04

In the next section, we present an alternative approach to characterizing the degree of irregularity in time series based on the concept of generalized entropy following the information theoretical framework described in Section 3.2.5. In this study, we show for the first time how such an approach can provide useful information on fluctuation dynamics in complex plasmas.

5. PAIR CORRELATION FUNCTION

A standard technique to characterize spatial ordering is to use the particle-particle pair correlation function, $g(r) = n(r)$/(total particles number $\times$ particle density $\times$ annular area enclosed), where $n(r)$ is the number of particles located inside a concentric annular ring of radius *r* from a center particle. The pair correlation function *g*(*r*) measures the translational order of the particle ensemble where series of peaks in the *g(r)* plot indicate the presence of periodicity. In the *g*(*r*) plot, the radius is normalized by inter-particle distance (ipd).

The corresponding pair-correlation functions for these particle configurations are shown in Figure 4. At pressure 0.441 mbar, 0.591mbar and 0.696 mbar, the distinctive peaks at the first nearest neighbor distance of *g*(*r*) plot suggesting the presence of short-range order as expected in the disordered liquid state. While at pressures 0.141 mbar and 0.291 mbar, pair correlations show no distinctive peak, which indicates the lack of periodicity in the particle arrangement, typical of disorder gas state.

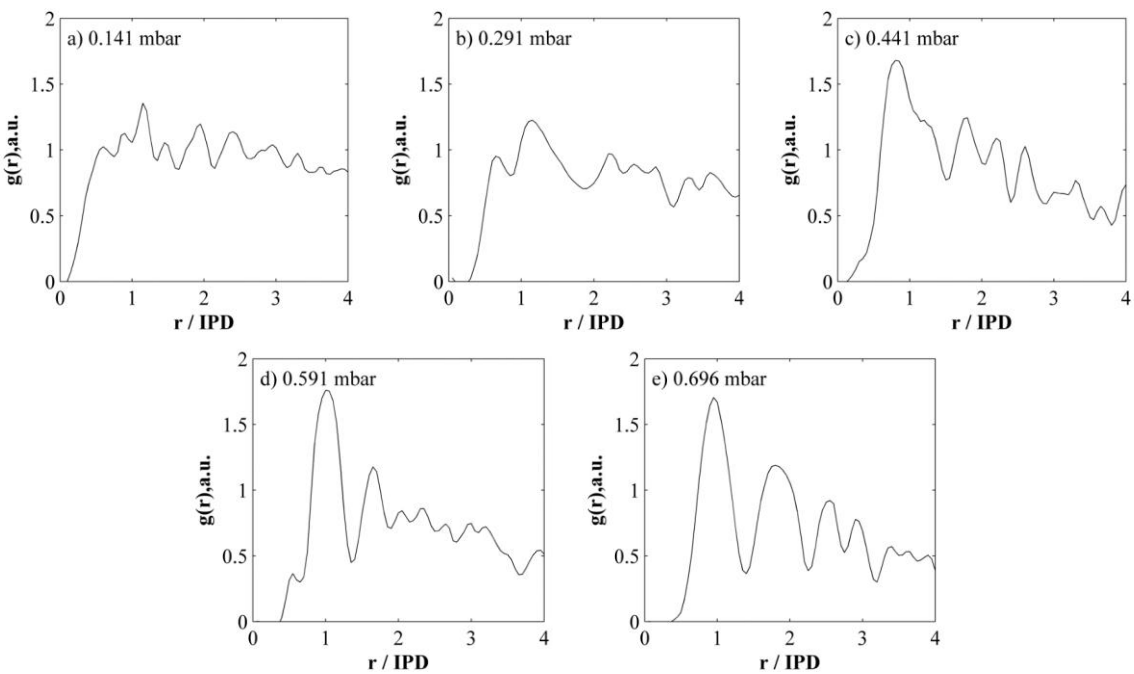

FIGURE 4. The pair correlation function *g*(*r*) of the dust particles at different pressures.

6. MEAN SQUARE DISPLACEMENT ANALYSIS

The advantage of direct observation of dust particles using high-speed video camera is the possibility of capturing the detailed motions of many individual particles. By having multiple video cameras to capture x-y and x-z planes, one is able to construct three-dimensional motion. The discharge chamber used in this experiment is however, very respective and only allow the video imaging in one plane (with the camera giving the top view). This will also limit the accuracy of the analysis. Despite this constraint, we have performed a detailed study of the particle trajectories and calculated the mean square displacement of particles. The slope of the log MSD versus log (lag-time, t) will give the MSD scaling exponent, α. The MSD scaling exponent α is related to H_{MSD} via the relation $\alpha=2H$. This is possible if one associate the particle motion to resemble fractional Brownian motion.

For a lower pressure of 0.141 mbar and 0.292 mbar, the particle can only be tracked up to 100 image frames due to rapid motion of the dust particle dispersing out of imaging view window. For higher pressures, more frames up to 1000 can be obtained allowing longer observation time because the particles seem to disperse slower. The trajectories of the dust particles at different pressures are shown in Figure 5. MSD was calculated using the relation discussed in Section 3.3.2 and the results are shown in Figures 4.22 -4.26 for different pressures. One noticeable feature among all the MSD plots in this study is the existence of bi-scaling behaviour in the MSD at all gas pressures. The scaling exponents at short lag-time are different from the scaling exponents at longer lag-time with a cross-over time, t_c. We found the particles exhibit super-diffusive transport (with $H_{\mathrm{MSD}} > 0.5$) at short lag-time for all the pressure. This finding is in agreement with other studies [22]. The particles move fast at short time and able to gain high speed and travel a greater distance. It then slows down to sub-diffusive behavior ($H_{\mathrm{MSD}} < 0.5$) after a cross-over time, t_c due to collisions with other dust particles.

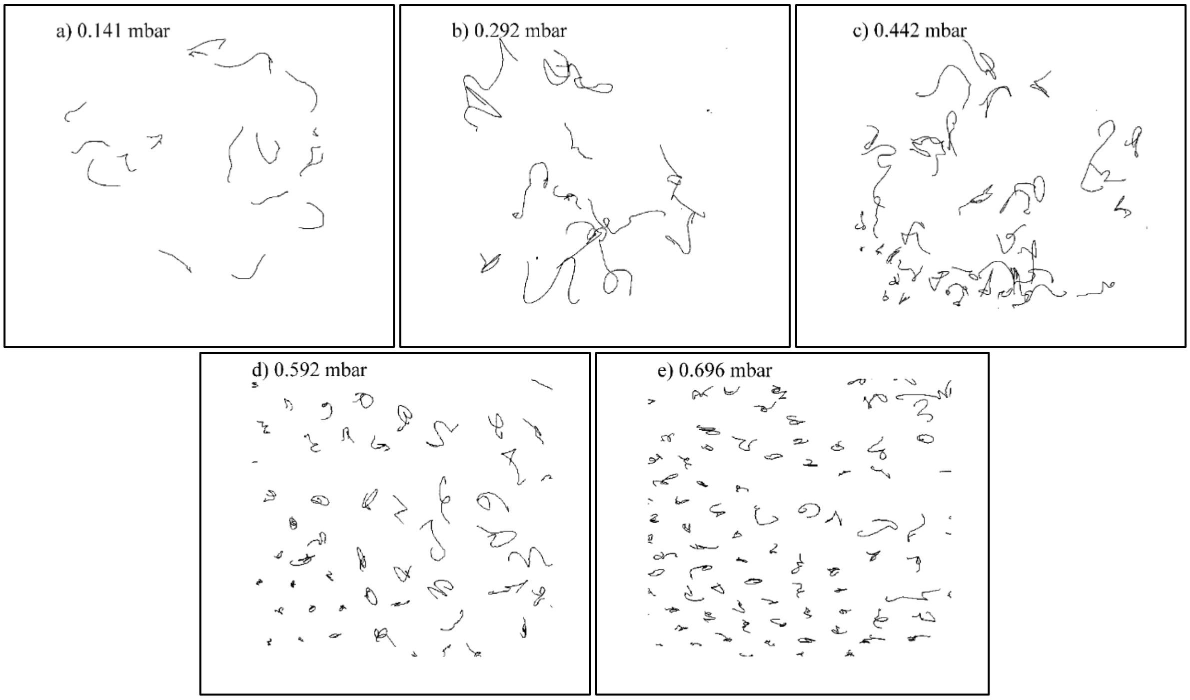

FIGURE 5. The trajectories of dust particles at different pressures a) 0.141 mbar, b) 0.292 mbar, c) 0.442 mbar, d) 0.592 mbar and e) 0.696 mbar.

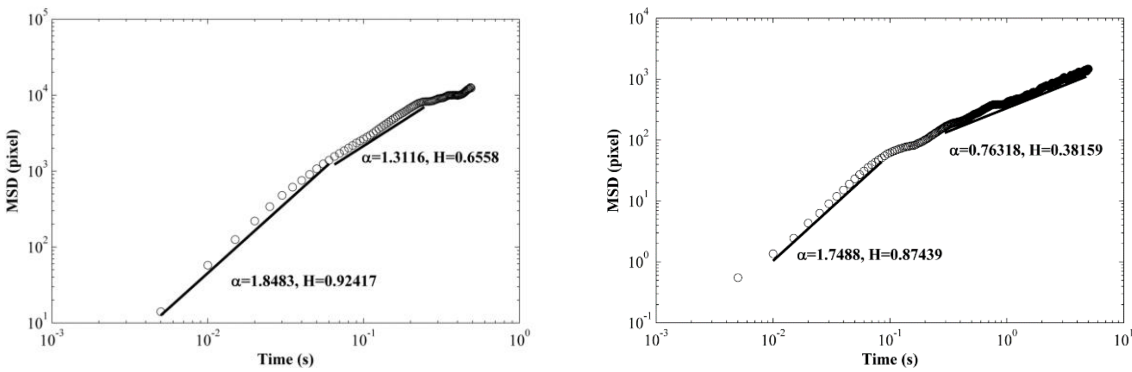

FIGURE 6. Means square displacement analysis for pressure 0.696 mbar.

Key transport characteristics associated with MSD analysis are summarized in Table 4.4. We notice the difference in MSD behaviour low pressure as compared to high pressure. For high pressure, there is a little bump after time transition. The little bump of MSD slope is due to the effect of caging as reported by Nunomura [9]. The transition from very fast superdiffusive to mild super-diffusive transport (near diffusive) occurs at a low pressure of 0.141 mbar within short cross-over time. For higher pressures, the transition is from super-diffusive to sub-diffusive altogether, but the switch took a longer time.

The damping effect in the kinetic energy comes largely from the collision with neutral gas at higher gas pressures. The change of super-diffusion to sub-diffusion when the pressure increases can then be corroborated to the caging effect by the Coloumb potential which causes particle movement to be confined and slower.

TABLE 2. Key parameters from mean square displacement analysis at different gas pressures.

Pressure (mbar)	Hurst exponent H_{MSD} (short time-lag $t < t_c$),	Cross-over time, t_c (sec)	Hurst exponent, H_{MSD} long time-lag, $t > t_c$)
0.141 ± 0.001	0.92 ± 0.01	0.5 ± 0.1	0.66 ± 0.01
0.292 ± 0.001	0.91 ± 0.01	0.7 ± 0.1	0.42 ± 0.01
0.442 ± 0.001	0.87 ± 0.01	0.7 ± 0.1	0.39 ± 0.01
0.592 ± 0.001	0.90 ± 0.01	0.7 ± 0.1	0.46 ± 0.01
0.696 ± 0.001	0.87 ± 0.01	0.9 ± 0.1	0.38 ± 0.01

7. DISCUSSION

In this paper, we have presented an empirical investigation of particle dynamics and fluctuation complex dusty plasma in 13.5 MHz radio-frequency capacitively coupled gas discharge systems. The observation of structural states was performed by varying the argon pressure discharge in the range of 0.1 mbar to 0.7 mbar with constant power at 50 W. Once the charged dust clouds are in equilibrium floating above the lower electrode, measurement intensity fluctuation from dynamic light scattering of particle were measured and at the same time the particle clouds are observed using a high-speed video imaging system connected to the particle tracking software. Particle trajectories were constructed from the sequential image frames based on the video files.

The first approach was based on a fractal time series analysis of the intensity fluctuation from the dynamic light scattering data measured as photocurrent from the photodiode. We used a widely popular fractal stochastic model known as the fractional Brownian motion that provides the framework to related key power-law scaling exponents to the model parameter, namely the Hurst parameter. Established fractal parameter estimators such as power spectral density (PSD) and wavelet scalogram were used to estimate the Hurst parameter from the time series. It was found that the Hurst exponents obtained from PSD and wavelet scalogram implied persistent characteristics with $0.5< H <1$ (fast dynamics/super-diffusion) at low pressure (0.141 mbar). The fluctuations were observed to be antipersistence with $0 < H <0.5$ for higher pressures (0.292 mbar - 0.696 mbar), which can be associated to slow dynamics/sub-diffusion. An alternative measure of randomness based on approximate entropy (ApEn) was also used to examine DLS data and was found to be consistent with interpretation provided by the Hurst exponents obtained in the fractal analysis (Table 5.1).

The second part of the study was based on direct observation of the particles using video imaging to study particle motion in the spatio-temporal domain. The pair correlation function was used to study the structural phase of particles' configurations. Next, the transport properties of charge dust particles were investigated using MSD for different pressures. We found the presence of different scaling regimes for different time scales. In general, dust particles showed fast transport (super-diffusion) at short time scales and slow dynamics (sub-diffusion) at long time scales for all pressures. At intermediate time scales of 0.1 seconds to 0.5 seconds, scaling exponent $H_{MSD} = 0.69 \pm 0.01$ is estimated at pressure 0.141 mbar, implying a super-diffusive transport. Meanwhile, at pressure 0.292 mbar, 0.442 mbar, 0.592 mbar and 0.696 mbar, subdiffusive transport with $H_{MSD} = (0.31 - 0.47) \pm 0.01$ was observed. The possible dynamics of transports at different pressures are summarized in Table 5.1 with a comparison to the deduction obtained from DLS experiments.

On long time scales, we found dust particle transports are sub-diffusive in the dusty plasma that has liquid-like state and super-diffusive in the gas-like state. This was consistently explained using the mean squared displacement analysis. Sub-diffusion mostly occurs because of the caging wells created by neighbouring particles. This finding has been published in Safaai et al., (2013), and also supported by other studies [9,12]. All of these works studied transport behaviour in dusty plasma liquid. However, this result is in disagreement with work reported in [23] and [13] who showed superdiffusion behaviour at long-time scale.

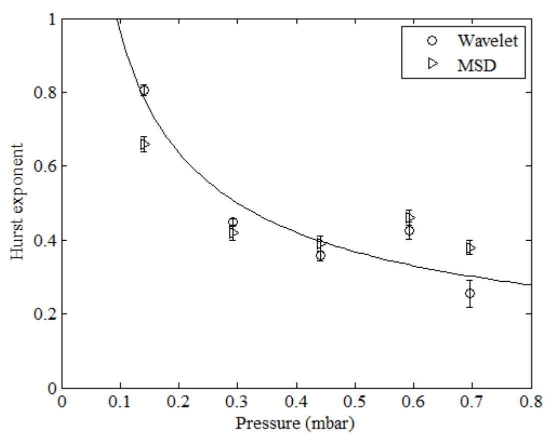

FIGURE 7. Comparison of Hurst exponents determined from DLS and MSD analysis.

When compared to a study on pair correlation analysis reported in [23], we infer that the dusty plasma at pressure 0.141 mbar is in the weakly coupled state, while at all other pressures, they are strongly coupled. The present study has provided new insights on the fluctuation dynamics in dusty plasmas covering both temporal and spatial perspectives.

TABLE 3. Comparison of transport characteristics (Hurst exponent) based on DLS and MSD analyses for different pressures.

Pressure (mbar)	DLS	MSD
0.141 ± 0.001	Persistence $H_{DLS} > 0.5$	Super-diffusive $H_{MSD} > 0.5$
0.292 ± 0.001 0.442 ± 0.001 0.592 ± 0.001 0.696 ± 0.001	Anti-persistence $H_{DLS} < 0.5$	Sub-diffusive $H_{MSD} < 0.5$

8. CONCLUSION

From this work, we were able to understand the scaling behaviour of DLS signal by comparing diffusion exponent from MSD of particle trajectories. DLS approach depends on collective effects, where the intensity measured by the photodiode is the sum of scattered light interfering with each other and fluctuating due to motion of particles. On the other hand, MSD analysis is an average of many individual particle trajectory. Both of these techniques have different approaches; however, we managed to show that both can be related based on scaling behaviour. We remark that the absolute values of the Hurst exponents reported in this study are relatively lower as compared to previous study published by the author on similar system. This is due to the thermal energy in the dust particles. The RF power from the previous work is greater with 100 Watt, while in this work we used only 50 W.

To summarize, fluctuation analysis of DLS signal was successfully carried out using fractal analysis to study complex changes in the particle configuration in a dusty plasma. The Hurst exponent determined from the DLS time series can be used to describe particle transport. The persistence value represents the fast dynamics and antipersistence value represents the slow dynamics.

We suggest the advantage of using fractal analysis for DLS time series as it provides an alternative way to identify the type of particle transport and this can be corroborated with MSD analysis. In some cases, it is even harder to estimate scaling exponent from MSD during the difficulty to observed the particle visually for long time in a given imaging window [13]. Understanding particle transport and the influence of scale invariance or power-law behaviour is important for predicting plasma behaviour in material processing and astrophysics plasma systems [5].

ACKNOWLEDGMENTS

This work was supported by the Malaysian Ministry of Higher Education’s Fundamental Research Grant Scheme (FP013-2014A) and Exploratory Research Grant Scheme (ER011-2011A). S.S Safaai acknowledges the Ministry of Higher Education and University Teknologi Malaysia for her PhD scholarship.

CONFLICT OF INTERESTS

The authors declare that there is no conflict of interests.

REFERENCES

[1] P. K. Shukla, A survey of dusty plasma physics. Phys. Plasmas, 8(5) (2001), 1791-1803.

[2] A. Piel, A. Melzer, Dusty plasmas-the state of understanding from an experimentalist's view. Adv. Space Res. 29(9) (2002), 1255-1264.

[3] S. V. Vladimirov, K. Ostrikov, Dynamic self-organization phenomena in complex ionized gas systems: New paradigms and technological aspects. Phys. Rep. 393(3) (2004), 175-380.

[4] R. L. Merlino, J. A. Goree, Dusty plasmas in the laboratory, industry, and space. Phys. Today, 57(7) (2004), 32-39.

[5] H. Thomas, G. E. Morfill, V. Demmel, J. Goree, B. Feuerbacher, D. Möhlmann, Plasma crystal: Coulomb crystallization in a dusty plasma. Phys. Rev. Lett. 73(5) (1994), 652-655.

[6] M. Nurujjaman, R. Narayanan, A. S. Iyengar, Continuous wavelet transform based time-scale and multifractal analysis of the nonlinear oscillations in a hollow cathode glow discharge plasma. Phys. Plasmas, 16(10) (2009), 102307.

[7] J. Zajac, E. Dufkova, V. Weinzettl, V. P. Budaev, S. Nanobashvili, Multifractal analysis of plasma turbulence in biasing experiments on Castor tokamak. Czechoslovak J. Phys. 55(12) (2005), 1615-1621.

[8] S. Nunomura, D. Samsonov, S. Zhdanov, G. Morfill, Self-diffusion in a liquid complex plasma. Phys. Rev. Lett. 96(1) (2006), 015003.

[9] W. T. Juan, I. Lin, Anomalous diffusion in strongly coupled quasi-2D dusty plasmas. Phys. Rev. Lett. 80(14) (1998), 3073-3076.

[10] L. J. Hou, A. Piel, P. K. Shukla, Self-diffusion in 2D dusty-plasma liquids: Numerical-simulation results. Phys. Rev. Lett. 102(8) (2009), 085002.

[11] S. Ratynskaia, C. Knapek, K. Rypdal, S. Khrapak, G. Morfill, Statistics of particle transport in a two-dimensional dusty plasma cluster. Phys. Plasmas, 12(2) (2005), 022302.

[12] V. E. Fortov, O. S. Vaulina, O. F. Petrov, et al. Transport of microparticles in weakly ionized gas-discharge plasmas under microgravity conditions. Phys. Rev. Lett. 90(24) (2003), 245005.

[13] J. Goree, B. Liu, Y. Feng, Diagnostics for transport phenomena in strongly coupled dusty plasmas. Plasma Phys. Control. Fusion, 55(12) (2013), 124004.

[14] J. D. Williams, Application of particle image velocimetry to dusty plasma systems. J. Plasma Phys. 82(3) (2016), 200-205.

[15] A. J. Hurd, P. Ho, Velocity persistence of Brownian particles generated in a glow discharge. Phys. Rev. Lett. 62(26) (1989), 3034-3037.

[16] S. V. Muniandy, W. X. Chew, C. S. Wong, Fractional dynamics in the light scattering intensity fluctuation in dusty plasma. Phys. Plasmas, 18(1) (2011), 013701.

[17] A. Aschinger, J. Winter, Dynamic light scattering study of phase transitions in three-dimensional complex plasmas. New J. Phys. 14(9) (2012), 093036.

[18] V. E. Fortov, V. I. Molotkov, A. P. Nefedov, O. F. Petrov, Liquid-and crystallike structures in strongly coupled dusty plasmas. Phys. Plasmas, 6(5) (1999), 1759-1768.

[19] H. M. Anderson, S. B. Radovanov, Dynamic laser light scattering studies of dusty plasmas in the Gaseous Electronics Conference Reference Cell. J. Vacuum Sci. Technol. A., Vac. Surf. Films, 14(2) (1996), 608-614.

[20] D. Blair, E. Dufresne, The Matlab Particle Tracking Code. Retrieved June 20, 2013, from http://physics/georgetown.edu/matlab. (2008).

[21] S. S. Safaai, S. V. Muniandy, W. X. Chew, et al. Fractal dynamics of light scattering intensity fluctuation in disordered dusty plasmas. Phys. Plasmas, 20(10) (2013), 103702.

[22] B. Liu, J. Goree, Superdiffusion in two-dimensional Yukawa liquids. Phys. Rev. E, 75(1) (2007), 016405.